Organic & Biomolecular Chemistry

Cite this: *Org. Biomol. Chem.*, 2012, **10**, 2263

www.rsc.org/obc

PAPER

An alternative approach: a highly selective dual responding fluoride sensor having active methylene group as binding site†

Priyadip Das, Manoj K. Kesharwani, Amal K. Mandal, Eringathodi Suresh, Bishwajit Ganguly* and Amitava Das*

Received 29th October 2011, Accepted 4th January 2012
DOI: 10.1039/c2ob06815j

A newly designed phosphonium derivative (**L**) having active methylene functionality, shows unusual preference towards F^- over all other anions. The binding process through C–H···F^- hydrogen bond formation was probed by monitoring the changes in either electronic or luminescence spectra. Changes in both cases are significant enough to allow visual detection. The loss of molecular flexibility of **L** on forming **L**·F^- effectively interrupts the non-radiative deactivation pathway and accounts for the observed *switch on* fluorescence response. The results of the time-resolved emission studies for **L** and **L**·F^- using a time-correlated single photon counting technique further corroborate this presumption. The excellent preference of **L** towards F^- is attributed to an efficient hydrogen bonding interaction between the strongly polarized methylene protons and F^-, which delineates the subtle difference in the affinity among other competing anionic analytes like CN^-, $H_2PO_4^-$, $CH_3CO_2^-$, *etc.* The relative affinities of various anions and the preferential binding of F^- to reagent **L** are also rationalized using computational studies.

Introduction

The binding of an ionic guest molecule to a molecular receptor is expected to induce an appreciable perturbation in the electronic environment of the host molecule. These binding-induced processes influence the spectral and/or redox behaviour of molecular receptors. Often these responses are sensitive enough to provide information about concentration gradient and relative affinity towards a specific analyte. Considering the fundamental roles of anions in various industrial, chemical, biological and environmental processes, research in the area of anion recognition and sensing has experienced exponential growth during the past decade. The design and synthesis of anion sensors capable of converting the anion binding event into a readable signal output through optical, electrochemical and magnetic resonance responses have received considerable attention.[1] In this regard, ligand engineering has introduced more systematic approaches for the development of tailor-made artificial receptors for anion detection, which are expected to have enormous significance in the areas of molecular recognition, environmental/biological sample analysis and diagonistics.[2] Over the past decades various neutral receptors, like urea, thiourea, imidazole, indole, amine, amide, pyrrole, phenol, and sulphonamide moieties with hydrogen bond donor functionalities and a Lewis acid in the recognition sites have been used for anion sensing studies.[3] On the other hand, cationic receptors for anion recognition[4] are generally derived from ammonium, guanidium, quinolinium, and protonated quinoxaline salts, where electrostatic interaction between the anionic guest and cationic receptors has been utilized. More recently, metal–anion coordination in appropriately functionalized metal complexes has also been used for the quest of finding receptors with desired specificity for certain anionic analytes.[5] A recent report also reveals that weaker interactions, like anion–π interaction, could also account for an improved sensitivity towards anions.[6] In certain anion recognition processes, where weaker interactions like hydrogen bonding and/or anion–π interaction(s) is/are operational, the relative affinity of a receptor towards different anions could be correlated based on the geometry of the receptor and/or anion itself and the basicity of the anions.[7] Because of the recent emphasis on the development of chromogenic sensors for anions with obvious ease in the detection processes, most synthetic sensor molecules generally involve the covalent linking of an optical signalling fragment to a neutral or cationic receptor for anions, which provides one or more H-bond donor sites for selective binding and sensing of some anions, especially F^-, $CH_3CO_2^-$, CN^-, $H_2PO_4^-$ and $PhCO_2^-$ in organic aprotic solvents.[2,3,8] Unfortunately, few colorimetric anion sensors are able to

Central Salt & Marine Chemicals Research Institute, Bhavnagar, 364002 Gujarat, India. E-mail: ganguly@csmcri.org, amitava@csmcri.org; Fax: +91 2782 567562; Tel: +91 2782 5677601

† Electronic supplementary information (ESI) available: Characterization data for **L**, analysis of the spectroscopic titration of **L** with different anions (Benisi–Hildebrand and titration plots), different excitation spectra in presence of F^- and CN^-, ESI-Mass spectra for binding stochiometry, ^1H and ^{31}P NMR study. CCDC 827147. For ESI and crystallographic data in CIF or other electronic format see DOI: 10.1039/c2ob06815j

delineate between these anionic substrates with comparable basicity and surface charge density.[9]

Among various anionic analytes, studies on the design of an efficient receptor for F^- have received considerable attention due to its deleterious influence in environmental pollution and significance in biology. F^- is a common ingredient in anaesthetic/hypnotic/psychiatric drugs and military nerve gases and is a contaminant in drinking water. Excess fluoride exposure may cause collagen breakdown, bone disorders, thyroid activity depression, immune system disruption and anaemia.[10] Thus, the need for fast and reversible binding for the real time monitoring of F^- and its accurate and specific recognition over all other competitive anions (*e.g.* $CH_3CO_2^-$, CN^-, $H_2PO_4^-$ and $PhCO_2^-$) has become an unfortunate reality.

In contrast to the well acknowledged hydrogen bond donor motifs which are generally used for anion recognition studies, we are reporting herein a simple phosphonium ion derivative (**L**) with acidic methylene groups, which acts as atypical hydrogen bond donors towards various anions. This receptor, **L** has a naphthalene skeleton as the building block as well as the signalling unit. The preferential binding and recognition of F^- are achieved through the strong H-bonding interaction (C–H···F^-) between the acidic methylene hydrogens (–CH_2–) of **L** and F^-. The present study reveals a rare example of the use of an active methylene functionality as a binding site for anion recognition.[9e] The selectivity for F^- over other anions, especially CN^-, $CH_3CO_2^-$ and $H_2PO_4^-$, is important as many reported F^- sensors suffer from the deleterious interference of these anions. This newly synthesized reagent (**L**) showed unique selectivity towards F^- over other common anionic analytes, including CN^-, and other oxygen-containing anions *e.g.* $CH_3CO_2^-$, $PhCO_2^-$ and $H_2PO_4^-$. The influence of the spatial orientation of the methylene hydrogens on the binding mode was rationalized on the basis of DFT studies.

Results and discussion

Receptor **L** was synthesized following the methodology shown in Scheme 1. 2,3-Dimethyl naphthalene (**1**) was allowed to react with *N*-bromosuccinimide (NBS) and converted to its corresponding di-bromo derivative. The crude reaction product was further purified by column chromatography to isolate **2** in the pure form with reasonable yield. This (**2**) on treatment with triphenylphosphine yielded **3** with Br^- as two counter anions, which was subsequently converted to the hexafluorophosphate salt (**L**) for further use. All intermediates and **L** were

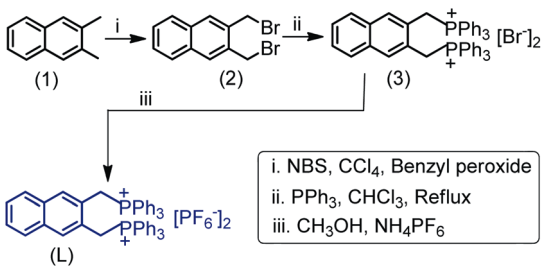

Scheme 1 Methodology adopted for the synthesis of **L**.

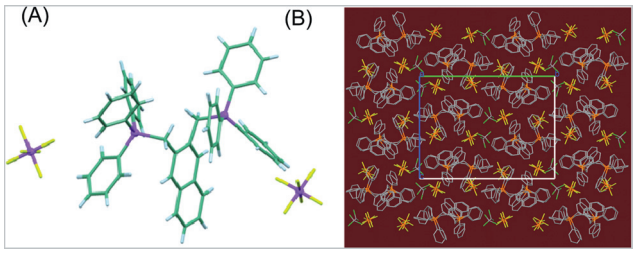

Fig. 1 (A) PLUTO diagram depicting the single crystal X-ray structure of one of the **L** moieties present in the asymmetric unit. (B) Packing diagram of the hexafluorophosphate salt of **L** viewed down the *a*-axis (hydrogen atoms are omitted for clarity).

characterized by standard spectroscopic techniques (see the Experimental section). The proposed molecular structure for **L** was also confirmed from the single crystal X-ray structure (Fig. 1).[11]

The receptor **L** crystallizes in a monoclinic system ($P2_1/c$ space group) with two molecules of the organic phosphonium dication and PF_6^- as counter anions in the asymmetric unit along with two $CHCl_3$ molecules as solvent of crystallization. The packing diagram viewed down *a*-axis is shown in Fig. 1B. As depicted in Fig. 1B, the organic dication present in the asymmetric unit is aligned down the *a*-axis and oriented diagonal to the *bc*-plane. $[PF_6]^-$ anions and lattice $CHCl_3$ molecules are between the adjacent phosphonium dications oriented diagonally. In fact, no classical H-bonding interaction is observed in **L**. However, C–H···F interaction between the fluorine atom as an acceptor from all PF_6 anions and phenyl hydrogens of the PPh_3^+ do exist with C···F distance ranging from 3.254(10) to 3.338(13) Å and C–H···F angles ranging from 149 to 176°, stabilizing the organic salt in the crystal lattice.

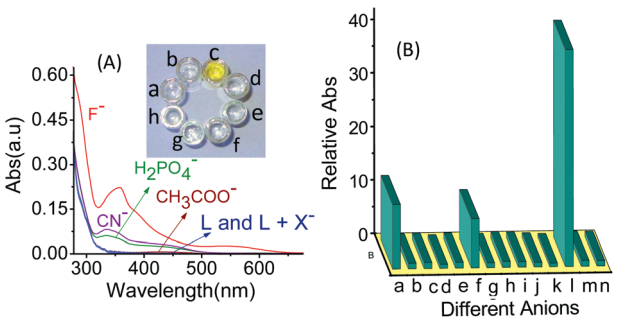

Fig. 2 (A) UV-Vis spectra of **L** (4.0×10^{-5} M) in the presence of $[Bu_4N]$-salts of various anions (8.0×10^{-4} M) (X^- = Cl^-, Br^-, I^-, CN^-, SCN^-, HSO_4^-, NO_2^-, NO_3^-, N_3^-, CH_3COO^-, ClO_4^-, IO_4^-, $PhCO_2^-$); inset: colour of the solution of **L** in acetonitrile with different anions: (a) **L**, (b) Cl^- or Br^-, (c) F^-, (d) HSO_4^-, (e) N_3^-, (f) $CH_3CO_2^-$, (g) CN^-/$H_2PO_4^-$, (h) $PhCO_2^-$; (B) UV response of **L** (4.0×10^{-5} M) in CH_3CN medium on addition of the solution of tetrabutyl ammonium salt of various anions (8.0×10^{-4} M): (a) CN^-, (b) ClO_4^-, (c) $PhCO_2^-$, (d) IO_4^-, (e) N_3^-, (f) $H_2PO_4^-$, (g) I^-, (h) Br^-, (i) $CH_3CO_2^-$, (j) Cl^-, (k) NO_3^-, (l) F^-, (m) HSO_4^-, (n) **L** with λ_{mon} = 358 nm.

UV-Vis study

Electronic spectra for **L** were recorded in CH_3CN solution in the absence and presence of tetrabutyl ammonium salts of common anionic analytes such as F^-, $H_2PO_4^-$, $CH_3CO_2^-$, Cl^-, Br^-, I^-, CN^-, SCN^-, HSO_4^-, NO_3^-, NO_2^-, N_3^-, ClO_4^-, $PhCO_2^-$ and IO_4^- (Fig. 2A). The absorption spectrum for **L** was featureless and no distinct absorption band was observed. A shoulder at 288 nm was observed and this could be ascribed to a charge transfer transition, which is typical for naphthalene-based chromophores.[12] Electronic spectra for **L** remained unchanged in the presence of excess (20 mole equivalents) of the above mentioned anionic analytes, except for F^-, CN^- and $H_2PO_4^-$. Among these anions, the changes were less significant for CN^- and $H_2PO_4^-$. Changes in the absorption spectra for CH_3COO^- could barely be detected. For F^-, an appreciable change was observed. A new absorption band at 357 nm, a shoulder at 283 nm and a relatively weaker, but broad, absorption band appeared at 541 nm upon addition of the solution of $[Bu_4N]F$ (TBAF) (Fig. 2A). The 283 nm band was ascribed to the naphthalene-based charge transfer (CT) transition, while new absorption bands at 357 and 541 were attributed to two different CT transitions involving naphthalene and F^- as donor fragment and the cationic $[PPh_3]^+$ moiety as the acceptor unit. Substantial changes in the absorption spectra signified a stronger interaction between the receptor **L** and F^-; however, a much weaker interaction for CN^-, $H_2PO_4^-$ and CH_3COO^- was observed (Fig. 2A). For all other anions, the absence of any change in absorption spectral pattern either suggests no interaction with **L** or that the interaction of the respective anions with **L** is too weak to perturb the energies of the frontier orbitals of the receptor molecule. Such a situation was further examined by ^1H NMR studies and the results of such studies are discussed latter. Spectral changes for **L** in the presence of TBAF were significant enough in the visible region to induce a visually detectable change in solution colour from colourless to yellow. The observed changes in solution (in acetonitrile) colour for **L** upon addition of 10 molar equivalents of tetrabutyl ammonium salts of respective anions are shown as an inset in Fig. 2A. This clearly reveals that aside from F^-, no colorimetric response was observed for addition of any other anions in CH_3CN solution of **L** in comparable concentration.

In order to evaluate the relative affinity of the respective anions (*e.g.* F^-, CN^-, $H_2PO_4^-$ and CH_3COO^-) towards **L**, systematic spectrophotometric titrations were carried out in acetonitrile medium with varying concentration of each one of these four anionic analytes, while maintaining the concentration of **L** at 4.0×10^{-5} M. On the basis of the UV-Vis titration profile (Fig. 3A) in the presence of externally added F^-, an association constant (K_A) of $(1.18 \pm 0.05) \times 10^4$ M^{-1} was obtained and 1 : 1 binding stoichiometry was obtained from the Benesi–Hildebrand plot. This was further confirmed from the Job's plot and ESI-MS analysis (ESI†). Analogously, the binding affinities for CN^-, $H_2PO_4^-$ and CH_3COO^- towards **L** were also evaluated and respective values were found to be $(3.22 \pm 0.2) \times 10^2$ M^{-1}, $(1.56 \pm 0.11) \times 10^2$ M^{-1} and 47 ± 7 M^{-1}. The binding of 1 : 1 for CN^- and $H_2PO_4^-$ was also confirmed from the Benesi–Hildebrand plot and Job's plot analysis (ESI†). Comparison of these data revealed that the binding affinities of CN^- and $H_2PO_4^-$ towards **L** were 37 and 75 times less than that for F^-, while that for CH_3COO^- was less by two orders of magnitude (~260 times).

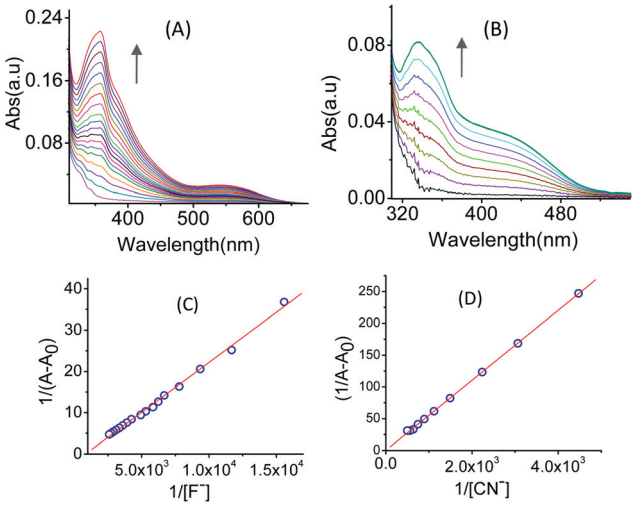

Fig. 3 Systematic changes in UV-Vis spectra of **L** (4.0×10^{-5} M) in CH_3CN with varying (A) $[F^-]$ ($0.0–6.0 \times 10^{-4}$ M), (B) with varying $[CN^-]$ ($0.0–1.78 \times 10^{-3}$ M); Benesi–Hildebrand plot of **L** with (C) fluoride ion, monitoring absorbance changes at 358 nm; (D) cyanide ion, monitoring absorbance changes at 420 nm. Good linear fit confirms the 1 : 1 binding stoichiometry.

The weaker binding of CN^- and $H_2PO_4^-$ was not sufficient to perturb the energies of the frontier orbitals of **L**, which accounts for the less or insignificant spectral changes. Hence, the dramatic combination of visually detectable colour change and specific response towards F^- makes this reagent ideally suited as a specific colorimetric sensor for F^- under the solution phase conditions employed. The observed unique specificity for F^- could be attributed to the highest charge density for F^- and consequently more efficient H-bond formation. Presumably, the increase in negative charge density on binding to F^- is expected to modify the dipoles associated with the charge transfer transition and/or stabilize the excited state of the chromophore, which could result in the significant changes in the observed UV-Vis spectrum and lead to a visually detectable colour change.

Luminescence study

We also studied the luminescence response of the receptor **L** in the absence and presence of F^-, $H_2PO_4^-$, $CH_3CO_2^-$, Cl^-, Br^-,

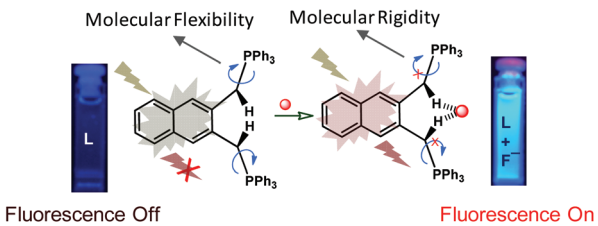

Scheme 2 Schematic representation of the increase in molecular rigidity on binding to an anion with associated changes in observed luminescence intensity for **L**.

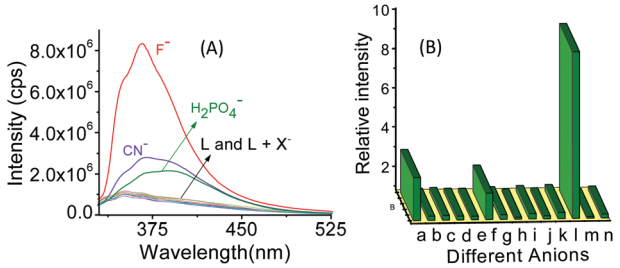

Fig. 4 (A) Fluorescence scanning of **L** (2.0×10^{-5} M) with [Bu_4N] salts of various anions (4.0×10^{-4} M) (X^- is Cl^-, Br^-, I^-, HSO_4^-, NO_2^-, NO_3^-, N_3^-, $CH_3CO_2^-$, ClO_4^-, IO_4^-, $PhCO_2^-$) and (B) luminescence response of **L** (2.0×10^{-5} M) in CH_3CN medium on addition of a solution of the tetrabutyl ammonium salt of various anions: (4.0×10^{-4} M): (a) CN^-, (b) ClO_4^-, (c) $PhCO_2^-$, (d) IO_4^-, (e) N_3^-, (f) $H_2PO_4^-$, (g) I^-, (h) Br^-, (i) $CH_3CO_2^-$, (j) Cl^-, (k) NO_3^-, (l) F^-, (m) HSO_4^-, (n) **L** with λ_{mon} = 366 nm and λ_{ext} = 280 nm.

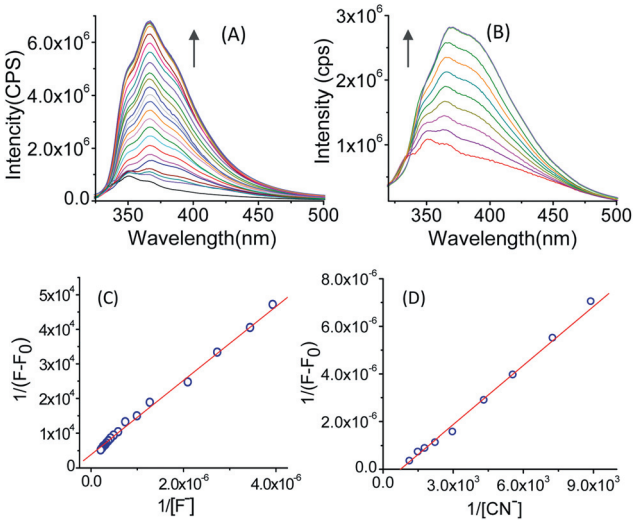

Fig. 5 Emission titration spectra (λ_{ext}: 280 nm, slit width 2/2 nm) of **L** (2.0×10^{-5} M) in CH_3CN with varying (A) [F^-] (0.0–3.15 $\times 10^{-4}$ M), (B) [CN^-] (0.0–9.0 $\times 10^{-4}$ M; Benesi–Hildebrand plot of **L** with (C) fluoride, monitoring emission intensity changes at 366 nm, and (D) cyanide ion, monitoring emission intensity changes at 370 nm. Good linear fit confirms the 1 : 1 binding stoichiometry.

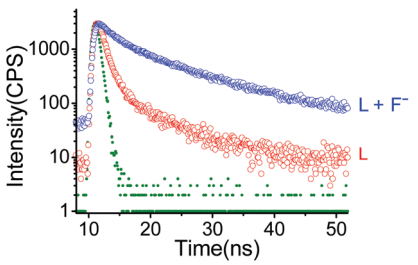

Fig. 6 Time-resolved decay profile for **L** (λ_{ext} = 280 nm, λ_{mon} = 366 nm) in the absence and presence of [Bu_4N]F (5 mole equivalents) in CH_3CN medium. Plot shown in green is laser source response.

I^-, CN^-, SCN^-, HSO_4^-, NO_3^-, NO_2^-, N_3^-, ClO_4^-, $PhCO_2^-$ and IO_4^- in acetonitrile medium. For the free receptor **L**, a weak emission band with emission maximum at 351 nm was observed on excitation at 280 nm. The emission quantum yield (Φ) for **L** was evaluated as 0.009 at λ_{max} = 351 nm with respect to naphthalene. The poor emission quantum yield for **L** could be explained based on its inherent molecular flexibility (Scheme 2), which favoured the non-radiative deactivation pathway of the naphthalene-based excited states. However, emission spectra recorded for **L** (2.0×10^{-5} M) in the presence of 20 mole equivalents of F^- in CH_3CN solution showed a "*turn-on*" emission response with 10 fold increase in the emission intensity at λ_{ems}^{max} = 366 nm (for λ_{ext} = 280 nm) (Fig. 4A), while these responses were much weaker for a solution of comparable concentration of either $H_2PO_4^-$ or CN^-.

The increase in emission intensity for an analogous experiment with CH_3COO^- was insignificant. Other anions failed to induce any detectable change in the emission spectral pattern of **L** (Fig. 4A). We further recorded the excitation spectra for **L**·F^- and **L**·CN^- using 366 nm as the emission band, which generated excitation spectra with absorption maxima at ~280 nm in both cases. Excitation at 357 nm resulted very weak and broad emission spectra with a maximum at ~440 nm, while no emission was observed on excitation at 540 nm, the other CT absorption band maximum (Fig. 2A). The results of the systematic analysis of the fluorescence titrations (Fig. 5A) also confirmed the binding stoichiometry of 1 : 1 (**L** : F^-) (Fig. 5C) with a binding constant of (1.25 ± 0.8) $\times 10^4$ M^{-1}. Equilibrium constants for the formation of **L**·CN^-, **L**·$H_2PO_4^-$ and **L**·CH_3COO^- were also evaluated from the emission titration profiles of the respective anions using an acetonitrile solution of **L** (2.0×10^{-5} M) in the presence of increasing [A^-] (A^- is CN^-/$H_2PO_4^-$/CH_3COO^-) and the respective values were found to be (3.32 ± 0.17) $\times 10^2$ M^{-1}, (1.76 ± 0.13) $\times 10^2$ M^{-1} and 59 ± 7 M^{-1}. Thus, the binding affinity of the respective ions toward **L**, obtained from emission titrations profiles for each of these four anions, matched well with the value obtained from the spectrophotometric analysis.

Relatively weaker binding affinities for ions like CN^-, $H_2PO_4^-$ and CH_3COO^- as compared to that for F^- ($K_{\mathbf{L}\cdot F^-} \gg K_{\mathbf{L}\cdot CN^-} \sim K_{\mathbf{L}\cdot H_2PO_4^-} \gg K_{\mathbf{L}\cdot CH_3COO^-}$) are reflected in their respective binding constants. Thus, detailed spectral studies revealed that the receptor **L** had a distinct preference towards F^-, as compared to CN^-, $H_2PO_4^-$ and all other common anions studied. An appreciable decrease in the molecular flexibility and associated increase in the emission quantum yield for the naphthalene-based emission band at 366 nm were also reflected in the results of time-correlated single photon counting studies (TCSPC) for **L** in the absence and presence of F^- using a 280 nm LED as an excitation source in an air equilibrated CH_3CN solution.

Emission decay traces for free **L** at λ_{mon} = 366 nm could be best fitted with bi-exponential time constants of τ_1 = 0.674 ± 0.008 ns (75%) and τ_2 = 4.013 ± 0.006 ns (25%) (Fig. 6). The longer and minor component could be attributed to the radiative decay of the naphthalene-based excited states, while the major component reflects the non-radiative deactivation of the excited state. However in the presence of 5 mole equivalents of F^-, decay traces could be best fitted to τ_1 = 1.35 ± 0.07 ns (20%) and τ_2 = 9.95 ± 0.08 ns (80%). The longer component became

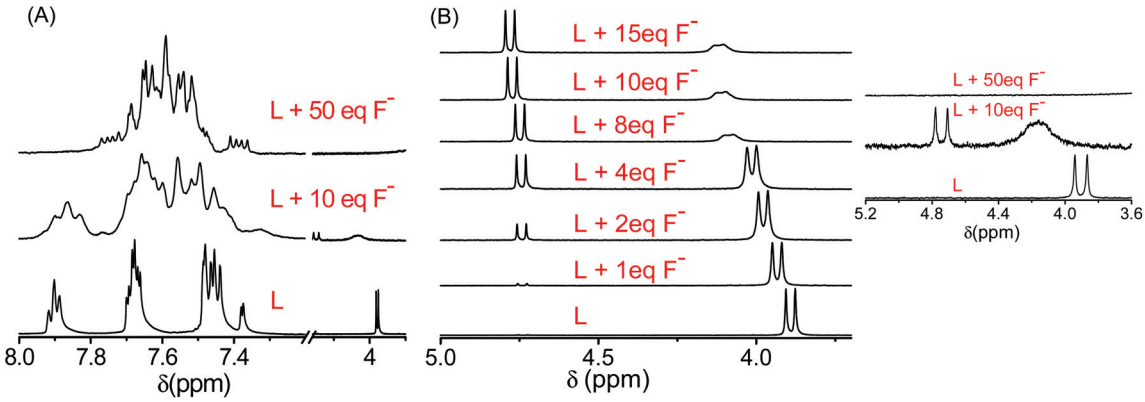

Fig. 7 Partial ^{1}H NMR spectra (A) of compound **L** in the absence and presence of 10 and 50 mole equivalents of F^- in CD_3CN, (B) showing changes in the position of the methylene proton signal in the absence and presence of varying [F^-] in CD_3CN; inset: showing changes in the methylene proton signal in the absence and presence of 10 and 50 mole equivalents of F^-.

the major one in the presence of F^- and this was attributed to the radiative decay pathway of the naphthalene-based excited states.

This clearly reveals that the enhancement in luminescence intensity could be attributed to the restricted vibrational and rotational relaxation modes of the non-radiative decay of **L**·F^-.

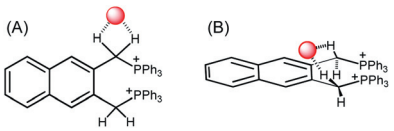

Scheme 3 Two probable binding modes for F^- for the **L**·F^- adduct formation.

^{1}H NMR study

The anion recognition property of **L** was also examined using ^{1}H NMR spectroscopy in CD_3CN medium, primarily by monitoring the changes in the signal of methylene proton (Fig. 7). ^{1}H NMR spectra of **L** were recorded in the absence and presence of various anions. For **L**, the signal for the –[CH_2]– functionality appeared as a doublet at δ = 3.90 ppm (J = 15 Hz) due to coupling with adjacent P-atoms and all aromatic protons appeared as multiplets within the region 7.917–7.374 ppm (Fig. 7A). The most noticeable change was observed only upon addition of 10 equiv. of [Bu_4N]F, while changes observed for comparable concentration of CN^- and $H_2PO_4^-$ were much less. For all other anions used in this study, either no change or insignificant changes were observed (ESI†). For F^-, significant downfield shifts of the methylene protons were evident, while the extent of those changes for CN^- and $H_2PO_4^-$ were small. In the case of Br^-, no change in the signals for the aromatic protons of **L** were observed and a slight upfield shift for the methylene protons was noticed (ESI†). This observation tends to suggest a strong ion-pair formation between the two cationic PPh_3-moieties and Br^-. Such an interaction was reported earlier for a phosphonium ion derivative and Br^-.[8b,13] This was further confirmed by ^{31}P NMR studies and is discussed latter. The H-bonding interaction between F^- and **L** was also investigated by systematic ^{1}H NMR titration (Fig. 7B).

As mentioned earlier, the signal for the four protons of two –[CH_2]– functionalities in **L** appeared as a doublet at δ = 3.90 ppm. This signifies that all four protons of the two –[CH_2]– functionalities are magnetically isotropic. The signal (doublet) for the four protons of the two –[CH_2]– functionalities shifted downfield (from 3.891 to 3.934 ppm) when one equivalent of F^- was added to a CD_3CN solution of **L**. This characteristic signal for $H_{[-CH_2-]}$showed a continuous downfield shift along with the appearance of another more downfield shifted ($\delta \geq 4.7$ ppm) doublet signal with increasing concentration of F^-. This change was associated with a decrease in intensity of the primary doublet signal with concomitant increase in intensity of the newly appeared downfield shifted doublet signal at $\delta \geq 4.7$ ppm, until [F^-] became 15 mole equivalents with respect to [**L**]. For even higher [F^-] (≥20 mole equivalents), the primary methylene proton signal was too broad to be studied properly. The coupling constant for the new doublet ($\delta \geq 4.7$) was also found to be 15 Hz, characteristic for the protons of the –[CH_2]– functionality coupled to adjacent P-atoms. Thus, four methylene protons became magnetically anisotropic upon binding to F^- and generated two sets of signals. The asymmetric influence tends to suggest an asymmetric binding of two of the four methylene protons to the F^-. Signals for several aromatic protons moved as multiplets to δ = 7.670–7.363 ppm (Fig. 7A) in the presence of excess F^-. Two different binding models could be envisaged that satisfy the 1 : 1 binding stoichiometry for **L**·F^- adduct formation (Scheme 3). Among these two possibilities, model B explained well the emission enhancement through gain in molecular rigidity and fits well with the observed shifts in the ^{1}H and ^{31}P NMR spectra. Formation of the C–H···F^- hydrogen bond in the adduct **L**·F^- would polarize the vicinal C–H bond of the methylene functionality, which is incidentally proximal to the cationic PPh_3^+ moiety. All these are expected to impart a certain partial double bond character for the bond that links the methyl C-atom and the P-atom of the $[P_{PPh_3}]^+$ unit, which consequently would have caused through-space deshielding effects on the other vicinal methylene protons and its observed distinct downfield shift.[9c] This result not only indicated that the receptor **L** is bound to F^- as an incipient hydrogen-bonded complex in the primary stage, but also supports the model B as the probable

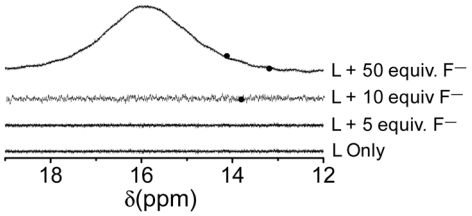

Fig. 8 ^{1}H NMR spectra of **L** in the absence and presence of varying concentrations of TBAF in CD_3CN, revealing the generation of HF_2^- due to deprotonation of **L** in the presence of 50 mole equivalents of TBAF in CD_3CN medium. Deprotonation of **L** or the generation of HF_2^- was not evident with 10 mole equivalents of TBAF.

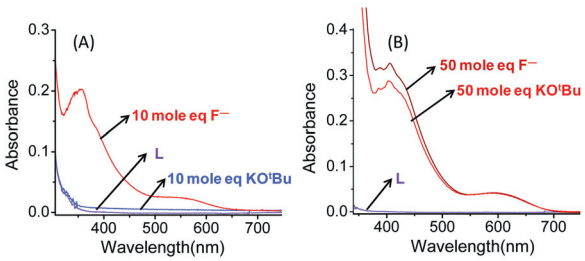

Fig. 9 Changes in the UV-Vis spectra of **L** (4.26×10^{-5} M) in the presence of (A) 10 mole equivalents of F^- and KO^{t}Bu, (B) 50 mole equivalents of F^- and KO^{t}Bu, in acetonitrile medium.

binding mode. For binding mode A (Scheme 3), one would not expect any significant downfield shift for the second set of methylene protons that are not hydrogen bonded to the F^-, a situation which is contrary to our experimental observation. However, in the presence of large excess (≥50 mole equivalents) of [F^-] deprotonation occurred and this was confirmed from the broad appearance of the ^{1}H NMR signal corresponding to HF_2^- at around 16 ppm[14] along with the disappearance of the characteristic doublet methylene signals (inset Fig. 7 and 8). The characteristic signal at around 16 ppm for HF_2^- was absent for [F^-] ≤15 mole equivalents.

This reflects the fact that in the presence of a large excess of F^- (≥50 mole equivalents) deprotonation of **L** occurs and the deprotonated species [$\mathbf{L}^-$] gets stabilized in a polar solvent like CH_3CN.[3e,7] The deprotonation process was also confirmed by UV-Vis spectroscopy. The absorption spectrum recorded for **L** showed two absorption maxima at 357 and 559 nm in the presence of 10 mole equivalents of F^- (Fig. 9A) due to the formation of the H-bonded adduct **L**·F^-. On further addition of excess F^- (50 mole equivalents), the absorption maxima shifted to 405 nm and 604 nm respectively (Fig. 9B). These changes were attributed to the deprotonation of **L**. This was further corroborated by the similarity of this spectrum to one recorded for **L** in the presence of 50 mole equivalents of KO^{t}Bu (Fig. 9B), which is certain to induce deprotonation. No significant spectral or colour change was observed when the spectrum for **L** was recorded in the presence of 10 mole equivalents of KO^{t}Bu (Fig. 9A). In order to clarify this further, ^{1}H NMR studies for **L** in the absence and presence of varying concentrations of KO^{t}Bu in DMSO (d_6) were also carried out. No change was observed in the spectrum that was recorded in the presence of 10 mole

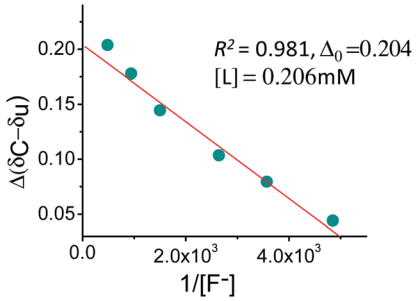

Fig. 10 A plot of $\Delta = (\delta_c - \delta_u)$ *vs.* 1/[F^-] for the ^{1}H NMR titration of **L** with F^- in CD_3CN.

equivalents of KO^{t}Bu; however, noticeable spectral changes were observed in the spectrum that was recorded in the presence of 50 mole equivalents of KO^{t}Bu. Signals for –[CH_2]– protons (at $\delta \sim 3.90$ ppm) completely disappeared, an observation which was analogous to that in the presence of F^- of comparable concentration. These results suggest the deprotonation of **L** in the presence of 50 mole equivalents of F^- as well as KO^{t}Bu.

The binding constant of F^- to receptor **L** through the H-bonded adducts formation was also evaluated from the ^{1}H NMR titration profile (Fig. 7B) using the following expression with **L** as host (H) and F^- as guest (G).

$$K_{ass} = (\Delta/(\Delta_0 - \Delta))/([G_0] - (\Delta/\Delta_0)[H_0])$$

Based on these NMR data, Δ_0, the difference in δ values for –[CH_2]– protons (δ_u for **L**) in the free form (*i.e.* **L**) and fully complexed species (δ_c for **L**·F^-) under solution phase, was determined by extrapolating the $\Delta = (\delta_c - \delta_u)$ *vs.* 1/[F^-] plot (Fig. 10). The value for Δ_0 was found to be 0.204 ppm and this was used for evaluation of $K_A^{F^-}$ (8589 ± 900 M^{-1}). This was within the error limit of the binding constant obtained from UV-Vis and emission titrations (*vide supra*).

The interaction of receptor **L** with F^- was also studied through ^{31}P NMR spectroscopy. The ^{31}P NMR spectrum of **L** in the absence and presence of 10 mole equivalents of F^- were recorded. A downfield shift of ~3 ppm for the $P_{[PPh_3]}^+$ signal of **L** was observed in the presence of F^- (Fig. 11). No such significant shift in the $P_{[PPh_3]}^+$ signal was observed in the presence of other common anions (Fig. 11 and ESI†). Contrary to our

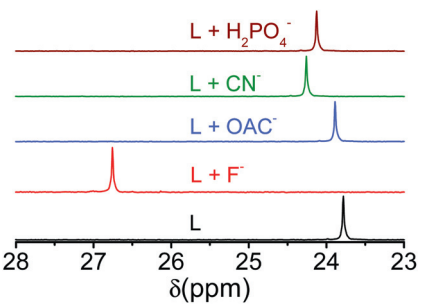

Fig. 11 ^{31}P NMR spectra of receptor **L** before and after addition of F^- (10 equiv.) and other anionic analytes $H_2PO_4^-$, OAc^- and CN^- (30 equiv.) in CD_3CN at room temperature.

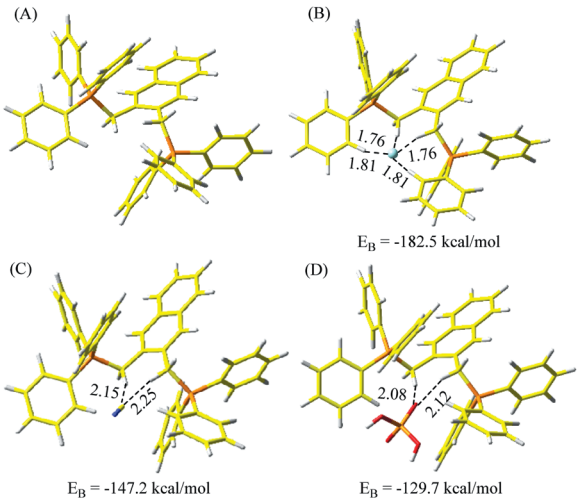

Fig. 12 GGA/BLYP/DNP optimized geometries and important distances (Å) of (A) **L**, (B) **L**·F^-, (C) **L**·CN^- and (D) **L**·$H_2PO_4^-$. Calculated binding energies (E_B) of anion complexes with **L** are also given. (yellow: C; red: O; cyan: F^-; orange: P; blue: N; white: H).

observations, an earlier report revealed an upfield shift of the $P_{[PPh_3]}^+$ signal of a phosphonium ion based receptor upon anion binding, and the upfield shift was attributed to a tight ion pair formation between Br^- and cationic phosphonium ion.[13] Thus, shifts observed in the present study described a well defined example of the use of acidic methylene functionality for anion recognition through H-bonded adduct formation and explain well the rigidity imparted on the receptor structure upon F^- coordination and thereby the increase in the naphthalene-based emission quantum yield for **L**.

Thus, these results indicate that the receptor **L** acts as a specific chromogenic sensor for F^- and presents an atypical example where methylene hydrogen atoms of the receptors **L** are involved in the formation of an effective hydrogen bonded adduct (**L**·F^-). The tendency of F^- to form stronger hydrogen bonds leads to its specific recognition among all other anions. The preferential binding of F^-, as compared to CN^- and $H_2PO_4^{2-}$, was also rationalized using computational studies.

To examine and rationalize the preferential binding of receptor **L** towards F^- anions as compared to CN^- and $H_2PO_4^-$, DFT calculations were performed. All geometries were optimized with GGA/BLYP/DNP methods[15] using the DMol3 density functional program (version 4.1.2) of Accelrys Inc.[16] The optimized geometry of receptor **L** is given in Fig. 12A. This was found to be in good agreement with the observed single crystal X-ray structure (Fig. 1A). The calculated and single crystal X-ray structures of **L** revealed that the active methylene hydrogens were positioned in such a way that only one analyte could effectively bind to the receptor. The other two active methylene hydrogens were oriented away from each other, and so were less likely to participate in the cooperative binding with the anions. The calculated binding affinity in the gas phase for 1 : 1 complexes of **L** with F^- ion was found to be -182.5 kcal mol^{-1}, which was higher than binding affinity with CN^- (-147.2 kcal mol^{-1}) and $H_2PO_4^-$ (-129.7 kcal mol^{-1}) ions (Fig. 12). These results suggest that F^- should have the preferential binding with receptor **L** compared to CN^- and $H_2PO_4^-$. This is in accordance with the experimental observations (*vide supra*). The F^- ion was positioned in a distorted square planar manner showing interaction with two active methylene hydrogens and two phenyl ring hydrogen atoms. The F^- ion interaction with the phenyl hydrogens is also supported by the change in ^1H NMR spectral pattern with F^- (*vide supra*).

Conclusions

In summary, we have successfully employed a phosphonium derivative of naphthalene **L** as a selective and sensitive sensor for F^-. Using this reagent (**L**) we have demonstrated a rational strategy, where acidic methylene functionality is effectively used for the selective detection of F^- over all other common anions (including CN^- and other oxy anions). This reagent was also found to be amenable to "*colour changing*" with associated "*turn-On*" fluorescence response. The higher selectivity for F^- among various anionic analytes can be attributed to the acidity of the methylene protons, and the high electronegativity and basicity of F^-. We have also investigated the interaction modes by detailed analysis of the NMR (^1H and ^{31}P NMR) and TCSPC experiments. The initial interaction modes of **L** with F^- in CH_3CN led to the formation of a hydrogen bonded adduct with associated changes in the absorption and emission spectral pattern; however, for F^- concentration > 50 mole equivalents with respect to the receptor **L**, deprotonation phenomena prevail.

Experimental section

NBS, 2,3-dimethyl naphthalene, dibenzoyl peroxide, tetrabutyl ammonium salt of various anions and ammonium hexafluorophosphate were obtained from Sigma-Aldrich and were used as received without any purification. Triphenyl phosphine and all the other reagents used were of reagent grade (S. D. Fine Chemical, India) and were used as received. Various analytical and spectroscopic data obtained for these intermediates provided necessary support for the proposed formulation and required purity. HPLC grade acetonitrile (Fisher Scientific) was used as a solvent. Chloroform, methanol and carbon tetrachloride used for different synthetic procedures and studies were purified through distillation following standard procedures prior to use. Microanalyses (C, H, N) were performed using a Perkin–Elmer 4100 elemental analyser. FTIR spectra were recorded as KBr pellets using Perkin-Elmer Spectra GX 2000 spectrometer. ^1H and ^{31}P NMR spectra were recorded on Bruker 200 MHz (Avance-DPX 200)/500 MHz (Bruker Avance II 500) FT NMR. Electronic spectra were recorded with Shimadzu UV-3101 PC spectrophotometer, while fluorescence spectra, as well as TCSPC studies were carried out using the Fluorolog HRIBA JOBIN YVON and Edinburgh Instruments, Model H5773-03, fitted with a blue-sensitive photomultiplier.

UV-Vis and fluorescence study

A 2.0×10^{-4} M solution of compound **L** (Scheme 1) in acetonitrile was prepared and stored in dark conditions. This solution was used for all spectroscopic studies after appropriate dilution.

2.0×10^{-3} M solutions of the tetrabutyl ammonium salt of the respective anions were prepared in predried and distilled acetonitrile and each solution was stored in an inert atmosphere. The solution of compound **L** was further diluted for spectroscopic titrations, and the effective final concentration was adjusted to 4.0×10^{-5} M, while the final analyte concentration for scanning was 8.0×10^{-4} M. The effective concentration of the solution of compound **L** used for the fluorescence study was 2.0×10^{-5} M, while the final analyte concentration during emission spectral scanning was 4.0×10^{-4} M. The $[Bu_4N]F$ solution was introduced in an incremental fashion during both the UV-Vis and luminescence titrations and their corresponding spectra were recorded at 298 K. Benesi–Hildebrand analyses were used to determine the association constant and binding stoichiometry.

Time-correlated single photon counting experiment

Time-resolved fluorescence measurements were carried out using Edinburgh Instruments, Model H5773-03. The instrument works on the principle of the TCSPC technique. The relative fluorescence quantum yields (ϕ_f) were estimated using eqn (1) in acetonitrile by using the integrated emission intensity of naphthalene ($\phi_f = 0.23$ in cyclohexane at RT) as a reference:[17]

$$\Phi_f = \Phi_f' \, (I_{sample}/I_{std})(A_{std}/A_{sample})(\eta^2{}_{sample}/\eta^2{}_{std}) \quad (1)$$

where Φ_f' is the absolute quantum yield for the naphthalene, used as reference; I_{sample} and I_{std} are the integrated emission intensities; A_{sample} and A_{std} are the absorbances at the excitation wavelength, and η_{sample} and η_{std} are the respective refractive indices.

Synthesis of 2 (2,3-dimethyl bromonaphthalene)

NBS (626 mg, 3.516 mmol) and a catalytic amount of recrystallized dibenzoylperoxide were added to a solution of **1** (250 mg, 1.60 mmol dissolved in 80 mL of CCl_4). The resulting mixture was refluxed for 4 h with irradiation from a 100 W lamp. The decomposed product of NBS was then separated by filtration and the filtrate was evaporated to dryness to afford an off-white coloured solid residue, which was subjected to column chromatography on silica gel as stationary phase and chloroform : hexane solvent mixture (1 : 1, v/v) as the eluent to get **2** as a pure product (380 mg, 75.5%). ^{1}H NMR (200 MHz, $CDCl_3$, 25 °C, TMS) δ (ppm): 7.86 (s, 2H; ArH), 7.815–7.809 (m, 2H; ArH), 7.519–7.512 (m, 2H; ArH), 4.882 (s, 4H; $-CH_2$). IR (KBr) ν_{max}/cm^{-1}: 3056, 1268, 1220, 1201, 773, 641, 633, ESI-MS (*m*/*z*): 338 (($M^+ + Na^+$), 50%). Elemental analysis: $C_{12}H_{10}Br_2$: calculated C (45.90), H (3.21); found C (46.21), H (3.01).

Synthesis of 3 (2,3-bis(triphenylphosphoniomethyl)naphthalene dibromide)

A solution of **2** (145 mg, 0.462 mmol) and triphenyl phosphene (233 mg, 1.016 mmol) in 50 mL dry chloroform was refluxed for 3–4 h, then the reaction mixture was allowed to stir at room temperature for 14 h. The reaction mixture was then evaporated to dryness to afford a thick oily residue, which was treated with diethyl ether and on constant stirring afforded a white solid residue, which was filtered off, dried properly and finally recrystallized from the minimum volume of chloroform to get the pure product **3** (341.8 mg, 88%). ^{1}H NMR (200 MHz, $CDCl_3$, 25 °C, TMS) δ (ppm): 7.970–7.871 (m, 11H; ArH), 7.776–7.677 (m, 17H; ArH), 7.439 (s, 2H; ArH), 7.366–7.269 (m, 6H; ArH), 5.739 (d, J = 14.8Hz, 4H; Ar–CH_2P). IR (KBr) ν_{max}/cm^{-1}: 3461, 3052, 2360, 1588, 1484, 1437, 1330, 1111, 1163, 996, 841, 747, 719, 690, 542, ESI-MS (*m*/*z*): 759 ((M^+–Br^-), 30%), 677.48 (($M^+ - 2Br^-$), 48%). Elemental analysis: $C_{48}H_{40}P_2Br_2$: calculated C (68.75), H (4.81); found C (67.85), H (4.73).

Synthesis of L (2,3-bis(triphenylphosphoniomethyl)naphthalene di(hexafluorophosphate)

To a solution of 0.40 g (0.109 mmol) of 2,3-bis(triphenylphosphoniomethyl)anthraquinone dibromide (**3**) in 20 mL of MeOH, NH_4PF_6 (0.465 g, 2.85 mmol) was added. The reaction mixture was stirred for 5 h, which afford a white precipitate. The white solid was collected by filtration and dried properly to give **L** 366 mg (79.5%). ^{1}H NMR (500 MHz, CD_3CN, 25 °C, TMS) δ (ppm): 7.91–7.88 (m, 6H; ArH), 7.70–7.66 (m, 12H; ArH), 7.48–7.44 (m, 16H; ArH), 7.38 (d, J = 3Hz 2H; ArH) 3.894 (d, J = 15Hz, 4H; Ar $-CH_2$P). ^{13}C NMR (500 MHz, CD_3CN, 25 °C, TMS) δ (ppm): 26.52 (d, Ar $-CH_2$P), 116.394, 123.838, 123.873, 127.205, 128.129, 130.234, 130.88, 132.436, 132.879, 134.102, 134.178, 135.676 (Ar– and P–Ar). IR (KBr) ν_{max}/cm^{-1}: 3433, 1589, 1440, 1112, 836, 741, 689, 556, 510, ESI-MS (*m*/*z*): 823 (($M^+ - PF_6^-$), 49%). Elemental analysis: $C_{48}H_{40}F_{12}P_4$: calculated C (59.51), H (4.16); found C (60.12), H (4.53).

Computational methods

All geometries were fully optimized with generalized gradient approximation (GGA) using BLYP functional integrated in density functional program DMol3 (version 4.1.2) of Accelrys Inc.[15,16] The physical wave functions are expanded in terms of numerical basis sets. We used a DNP double numerical polarized basis set which is comparable to the 6-31G** basis set. All calculations were performed in the gas phase.

Acknowledgements

DST and CSIR (India) have supported this work. P. D. and A. K. M. acknowledge CSIR, New Delhi, and M. K. K. acknowledges UGC, New Delhi for Sr. Research Fellowship.

Notes and references

1 (*a*) F. P. Schmidtchen and M. Berger, *Chem. Rev.*, 1997, **97**, 1609; (*b*) P. D. Beer and P. A. Gale, *Angew. Chem., Int. Ed.*, 2001, **40**, 486; (*c*) C. Suksai and T. Tuntulani, *Chem. Soc. Rev.*, 2003, **32**, 192; (*d*) R. Martínez-Máñez1 and F. Sancenón, *Chem. Rev.*, 2003, **103**, 4419; (*e*) R. Martínez-Máñez1 and F. J. Sancenón, *J. Fluoresc.*, 2005, **15**, 267; (*f*) T. Gunnlaugsson, M. Glynn, G. M. Tocci, P. E. Kruger and F. M. Pfeffer, *Coord. Chem. Rev.*, 2006, **250**, 3094; (*g*) J. W. Steed, *Chem. Commun.*, 2006, 2637; (*h*) M. H. Filby and J. W. Steed, *Coord. Chem. Rev.*, 2006, **250**, 3200; (*i*) P. A. Gale and R. Quesada, *Coord.*

Chem. Rev., 2006, **250**, 3219; (*j*) B. T. Nguyen and E. V. Anslyn, *Coord. Chem. Rev.*, 2006, **250**, 3118.
2 (*a*) P. D. Beer and P. A. Gale, *Angew. Chem., Int. Ed.*, 2001, **40**, 486; (*b*) J. L. Sessler, P. A. Gale and W. S. Cho, *Anion Receptor Chemistry*, RSC, Cambridge, 2006; (*c*) P. A. Gale, *Coord. Chem. Rev.*, 2001, **213**, 79; (*d*) S. O. Kang, J. M. Llinares, V. W. Day and K. B. James, *Chem. Soc. Rev.*, 2010, **39**, 3980; (*e*) R. M. Manez and F. Sancenon, *Chem. Rev.*, 2003, **103**, 4419; (*f*) J. W. Steed, *Chem. Soc. Rev.*, 2009, **38**, 506; (*g*) R. M. Duke, E. B. Veale, F. M. Pfeffer, P. E. Kruger and T. Gunnlaugsson, *Chem. Soc. Rev.*, 2010, **39**, 3936; (*h*) L. A. Joyce, S. H. Shabbir and E. V. Anslyn, *Chem. Soc. Rev.*, 2010, **39**, 3621; (*i*) *Supramolecular Chemistry of Anions*, ed. A. Bianchi, K. Bowman-James and E. Garcka-Espala, Wiley-VCH, New York, 1997; (*j*) F. P. Schmidtchen, *Coord. Chem. Rev.*, 2006, **250**, 2918; (*k*) V. Amendola, M. Vonizzoni, D. Esteban-Gomez, L. Fabbrizzi, M. Licchelli, F. Sancenón and A. Taglietti, *Coord. Chem. Rev.*, 2006, **250**, 1451.
3 (*a*) M. Cametti and K. Rissanen, *Chem. Commun.*, 2009, 2809; (*b*) P. A. Gale, S. E. G. Garrido and S. E. Garlic, *Chem. Soc. Rev.*, 2008, **37**, 151; (*c*) Q. Wang, Y. Xie, Y. Ding, X. Li and W. Zhu, *Chem. Commun.*, 2010, **46**, 3669; (*d*) D. A. Jose, D. K. Kumar, B. Ganguly and A. Das, *Org. Lett.*, 2004, **6**, 3445; (*e*) D. A. Jose, P. Kar, D. Koley, B. Ganguly, W. Thiel, H. N. Ghosh and A. Das, *Inorg. Chem.*, 2007, **46**, 5576; (*f*) X. He, S. Hu, Y. Guo, J. Xu and S. Shao, *Org. Lett.*, 2006, **8**, 331; (*g*) M. J. Chmielewski and J. Jurczak, *Chem.–Eur. J.*, 2005, **11**, 6080; (*h*) J. Yoo, M. S. Kim, S. J. Hong, J. L. Sessler and C. H. J. Lee, *J. Org. Chem.*, 2009, **74**, 1065; (*i*) C. Caltagirone, G. W. Bates, P. A. Gale and M. E. Light, *Chem. Commun.*, 2008, **61**; (*j*) D. Esteban-Gomez, L. Fabbrizzi and M. Licchelli, *J. Org. Chem.*, 2005, **70**, 5717; (*k*) V. Thiagarajan and P. Ramamurthy, *J. Lumin.*, 2007, **126**, 886.
4 (*a*) M. D. Best, S. L. Tobey and E. V. Anslyn, *Coord. Chem. Rev.*, 2003, **240**, 3; (*b*) J. M. Llinares, D. Powell and K. Bowman-James, *Coord. Chem. Rev.*, 2003, **240**, 57; (*c*) S. K. Kim, N. J. Singh, S. J. Kim, H, G. Kim, J. K. Kim, J. W. Lee, K. S. Kim and J. Yoon, *Org. Lett.*, 2003, **5**, 2083; (*d*) M. Melaimi and F. P. Gabbaie, *J. Am. Chem. Soc.*, 2005, **127**, 9680; (*e*) V. Amendola, L. Fabbrizzi and E. Monzani, *Chem.–Eur. J.*, 2004, **10**, 76; (*f*) R. Badugu, J. R. Lakowicz and C. D. Geddes, *J. Fluoresc.*, 2004, **14**, 693; (*g*) B.-g. Zhang, P. Cai, C. Y. Duan, R. Miao, L. G. Zhu, T. Niitsu and H. Inoue, *Chem. Commun.*, 2004, 2206; (*h*) S. Mizukami, T. Nagano, Y. Urano, A. Odani and K. Kikuchi, *J. Am. Chem. Soc.*, 2002, **124**, 3920; (*i*) M. S. Han and D. H. Kim, *Angew. Chem., Int. Ed.*, 2002, **41**, 3809.
5 (*a*) P. D. Beer, D. P. Cormode and J. Davis, *Chem. Commun.*, 2004, 414; (*b*) A. Labande, J. Ruiz and D. Astruc, *J. Am. Chem. Soc.*, 2002, **124**, 1782; (*c*) S. Watanabe, M. Sonobe, M. Arai, Y. Tazume, T. Matsuo, T. Nakamura and K. Yoshida, *Chem. Commun.*, 2002, 2866.
6 S. Guha and S. Saha, *J. Am. Chem. Soc.*, 2010, **132**, 17674.
7 (*a*) A. Ghosh, B. Ganguly and A. Das, *Inorg. Chem.*, 2007, **46**, 9912; (*b*) A. D. Jose, D. K. Kumar, B. Ganguly and A. Das, *Tetrahedron Lett.*, 2005, **46**, 5343; (*c*) A. Ghosh, A. D. Jose, B. Ganguly and A. Das, *J. Mol. Model.*, 2010, **16**, 1441; (*d*) A. D. Jose, D. K. Kumar, P. Kar, S. Verma, A. Ghosh, B. Ganguly, H. N. Ghosh and A. Das, *Tetrahedron*, 2007, **63**, 12007; (*e*) K. B. James, *Acc. Chem. Res.*, 2005, **38**, 671; (*f*) E. Galbraith and T. D. James, *Chem. Soc. Rev.*, 2010, **39**, 3831.
8 (*a*) E. J. Cho, B. J. Ryu, Y. J. Lee and K. C. Nam, *Org. Lett.*, 2005, **5**, 2627; (*b*) C. Bhaumik, S. Das, D. Saha, S. Dutta and S. Baitalik, *Inorg. Chem.*, 2010, **49**, 5049; (*c*) L. Wang, X. He, Y. Guo, J. Xu and S. Shao, *Org. Biomol. Chem.*, 2011, **9**, 752; (*d*) E. Quinlan, S. E. Matthews and T. Gunnalaugsson, *J. Org. Chem.*, 2007, **72**, 7497.
9 (*a*) Q. Wang, Y. Xie, Y. Ding, X. Li and W. Zhu, *Chem. Commun.*, 2010, **46**, 3669; (*b*) S. V. Bhosale, S. Bhosale, M. B. Kalyankar and S. J. Langford, *Org. Lett.*, 2006, **11**, 5418; (*c*) C-I. Lin, S. Selvi, J-M. Fang, P-T. Chou, C-H. Lai and Y-M. Cheng, *J. Org. Chem.*, 2007, **72**, 3537; (*d*) Z-H. Lin, S-J. Ou, C. Duan, B. Zhang and Z. Bai, *Chem. Commun.*, 2006, 624; (*e*) P. Das, A. K. Mondal, M. K. Kesharwani, E. Suresh, B. Ganguly and A. Das, *Chem. Commun.*, 2011, **47**, 7398.
10 (*a*) P. Connet, *Fluoride*, 2007, **40**, 155; (*b*) R. J. Carton, *Fluoride*, 2006, **39**, 163; (*c*) E. B. Bassin, D. Wypij and R. B. Davis, *Cancer, Causes Control*, 2006, **17**, 421; (*d*) Y. Yu, W. Yang, Z. Dong, C. Wan, J. Zhang, J. Liu, K. Xiao, Y. Huang and B. Lu, *Fluoride*, 2008, **41**, 134; (*e*) R. P. Schwarzenbach, B. I. Escher, K. Fenner, T. B. Hofstetter, C. A. Johnson, U. V. Gunten and B. Wehrli, *Science*, 2006, **313**, 1072.
11 Crystal data. **Compound 1** (CCDC 827147†): $C_{98}H_{82}Cl_6F_{24}P_8$, formula weight = 2176.10, Monoclinic, $P2_1/c$; a = 20.4538(12), b = 25.3853(15), c = 19.2348(12) Å, α = 90, β = 90.2290(10), γ = 90°, U = 9987.1(10) $Å^{-3}$, T = 293(2) K, Z = 4, D_c = 1.447 Mg m^{-3}, μ(Mo K_α) = 0.391 mm^{-1}, $F(000)$ = 4432, colourless block 0.46 × 0.32 × 0.20 mm; 43 845 reflections measured of which 14 757 were unique (R_{int} = 0.1229), 1225 parameters, R_1 = 0.1336, wR_2 = 0.2789 (with $I > 2\sigma(I)$), R_1 = 0.2090, wR_2 = 0.3180 for all data, GOF on F^2 S = 1.144, Largest diff. peak and hole = 0.797 and –0.529 e $Å^{-3}$.
12 N. J. Turro, V. Ramamurthy and J. C. Scaiano, *Modern Molecular Photochemistry of Organic Molecules by University Science Books*, Sausalito, California (USA), 2010.
13 A. Hamadi, K. C. Num, B. J. Ryu, J. S. Kim and J. Viceness, *Tetrahedron Lett.*, 2004, **45**, 4689.
14 (*a*) P. Ashokumar, V. T. Ramakrishnan and P. Ramamurthy, *Chem.–Eur. J.*, 2010, **16**, 13271; (*b*) Z. Xu, S. Kim, H. N. Kim, S. J. Han, C. Lee, J. S. Kim, X. Quan and J. Yoon, *Tetrahedron Lett.*, 2007, **48**, 9151; (*c*) X. Peng, Y. Wu, J. Fan, M. Tian and K. Han, *J. Org. Chem.*, 2005, **70**, 10524; (*d*) A. Ghosh, S. Verma, B. Ganguly, H. N. Ghosh and A. Das, *Eur. J. Inorg. Chem.*, 2009, 2496.
15 (*a*) J. P. Perdew, J. A. Chevary, S. H. Vosko, K. A. Jackson, M. R. Pederson, D. J. Singh and C. Fiolhais, *Phys. Rev. B: Condens. Matter*, 1992, **46**, 6671; (*b*) A. D. Becke, *J. Chem. Phys.*, 1997, **107**, 8554; (*c*) C. L. Lee, W. Yang and R. G. Parr, *Phys. Rev. B*, 1988, **37**, 785.
16 B. Delley, *J. Chem. Phys.*, 2000, **113**, 7756.
17 Reference materials for fluorescence measurement. D. F. Eaton, *Pure Appl. Chem.*, 1988, **60**, 1107.